Applied Catalysis B: Environmental 220 (2018) 553–560

Contents lists available at ScienceDirect

Applied Catalysis B: Environmental

journal homepage: www.elsevier.com/locate/apcatb

Alkaline modified g-C_3N_4 photocatalyst for high selective oxide coupling of benzyl alcohol to benzoin

Xiang Sun[a,b], Dong Jiang[a,1], Ling Zhang[a], Wenzhong Wang[a,*]

[a] State Key Laboratory of High Performance Ceramics and Superfine Microstructure, Shanghai Institute of Ceramics, Chinese Academy of Sciences, 1295 Dingxi Road, Shanghai 200050, PR China

[b] University of Chinese Academy of Sciences, Beijing 100049, PR China

ARTICLE INFO

Keywords:
C—C coupling
Photocatalysis
g-C_3N_4
Alkali modification
Benzoin

ABSTRACT

Benzoin is an important feedstock with high additional value for its extensive use in chemical industry. Benzoin condensation characterized by C—C coupling between benzaldehyde requires the use of nucleophilic catalysts including cyanide or *N*-heterocyclic carbene and is restricted to organic medium such as MeCN, diethyl ether, etc. Construction of efficient and non-toxic catalysts for benzoin synthesis still remains a challenge. Herein, highly selective (97%) benzoin synthesis from benzyl alcohol was achieved over potassium modified g-C_3N_4 via light-driven tandem selective oxidation and C—C coupling. The outstanding performance was attributed to alkali modifications on the electronic structure and surface chemical environment of g-C_3N_4. K^+ intercalation not only facilitated the light harvesting as well as the transport of charge carriers, but also induced surface deprotonation of g-C_3N_4 and thus remarkable nucleophilicity for prompting the C—C coupling reactions. This work sheds light on the design of earth-abundant inorganic photocatalysts for C—C coupling reactions such as the green synthesis of benzoin under ambient conditions.

1. Introduction

Benzoin is among the most important chemical feedstocks and high value-added downstream products, and has been used as versatile intermediates in the manufacture of various chemical additives, dyestuff, pharmaceuticals as well as the precursor of photoinitiator [1–4]. For the present, industrial benzoin synthesis from benzaldehyde coupling generally requires the catalysis of toxic cyanide (CN^-) or alternative organics with strong nucleophilicity (e.g. nitroalkanes, enamines, phosphonates, malonates, etc.) [5–10]. The bottleneck of benzoin condensation lies in the sluggish C—C bond formations between two benzaldehyde molecules, that is, the homo-benzoin process. In order to achieve efficient C—C coupling, umpolung of carbonyl carbon from one benzaldehyde molecule is of crucial importance. In this regard, organic medium (MeCN, diethyl ether, etc.) is usually required to stabilize the structure of catalysts for C—C coupling reaction, greatly hindering the application of most organ-catalysts [11]. Seeking suitable catalysts for benzoin condensation at ambient conditions towards minimal toxic emissions has an important practical significance.

Semiconductor photocatalysis has been developed as a novel approach to facilitate selective activation of specific chemical bonds during organics transformation, such as oxidation, nitration, coupling, and so on [12,13]. Graphite-like carbon nitride (g-C_3N_4), as a non-toxic and metal-free photocatalyst, has shown its peculiar potential in selective catalysis [14,15]. However, pure g-C_3N_4 suffers from poor performance far from satisfied for C—C coupling reaction, mainly due to the weak nucleophilicity of the active sites on g-C_3N_4, limited utilization of solar spectrum as well as the fast recombination of photo-induced electron-hole (e^-/h^+) pairs. In order to boost photocatalytic benzoin synthesis over g-C_3N_4, surface alkaline modification is believed to be the key [7]. On the one hand, introduced alkali atoms can increase the surface basicity of the photocatalysts as well as modify the electron structure of carbon atom in g-C_3N_4 to show nucleophilic property [16]. On the other hand, surface alkaline modification has exhibited the potential in enhancing the light-harvesting ability via narrowing the band gap of pristine host materials [17–20]. Given above inspirations, photo-induced nucleophilicity could be further expected over alkalinized g-C_3N_4, favorable for the C—C bond formation in benzoin synthesis.

In this study, K^+ modified g-C_3N_4 (denoted as Kn-CN, n = 1, 2, 3 n delegates the K^+ concentration) was synthesized via KOH solution immersing. Instead of benzaldehyde, benzyl alcohol which is economically more suitable was chosen as the starting material. Under Xe lamp irradiation at room temperature, K3-CN sample exhibited significant

* Corresponding author.
E-mail address: wzwang@mail.sic.ac.cn (W. Wang).
[1] Dong Jiang is the co-first author.

http://dx.doi.org/10.1016/j.apcatb.2017.08.057
Received 5 July 2017; Received in revised form 10 August 2017; Accepted 17 August 2017
Available online 31 August 2017

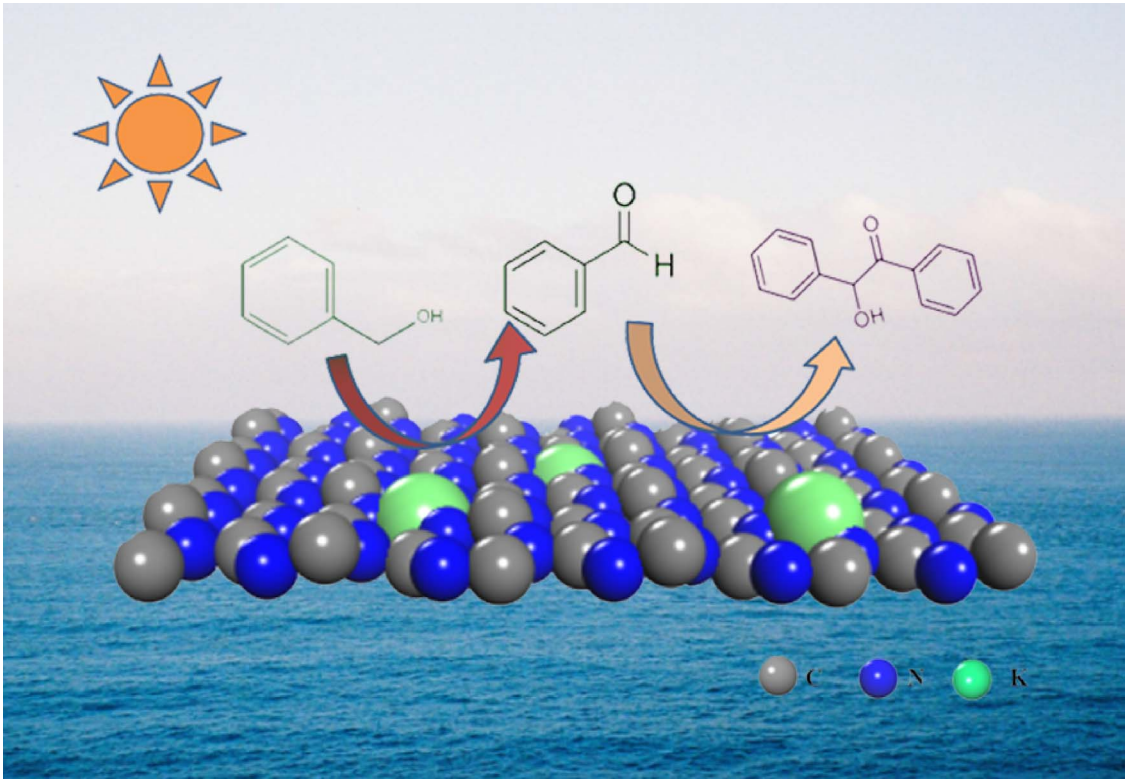

Scheme 1. C—C coupling for benzoin condensation over K—CN.

conversion (90.2%) and selectivity (97%) in transforming benzyl alcohol to benzoin, while for pristine g-C_3N_4 the selectivity and conversion are only 6.3% and 4.3%, respectively. Careful studies revealed that the benzoin synthesis consists of two successive processes (Scheme 1), i.e. selective benzyl alcohol conversion to benzaldehyde, followed by benzoin formation via C—C coupling between benzaldehyde. The superior performance of K—CN is mainly attributed to the twofold enhancement of alkali modification. Firstly, K intercalation facilitates the light harvesting of K—CN as well as the transport of interlayer electrons. Secondly, after alkaline treatment K—CN turned to present much enhanced nucleophilicity on the surface, greatly enhancing the C—C coupling between benzaldehyde molecules.

2. Experiment section

2.1. Sample preparation

All the reagents were purchased from Chemical Reagents Co., Ltd (Shanghai, China), and used without further purification. In a typical synthesis procedure, Melamine (5 g) in a covered crucible (10 mL) was heated in muffle furnace at 550 °C for 3 h under static air with a ramp rate of 10 °C/min. The K^+ modified g-C_3N_4 prepared with different concentration of KOH solution (1%, 2% and 5%) was labeled as K1-CN, K2-CN and K3-CN, respectively. The K doped g-C_3N_4 was synthesized by immersing the pristine g-C_3N_4 into KOH solution of known concentration with continuously agitation at 200 °C until the complete evaporation of water. The resulted powders were collected and rinsed with ultrapure water for several times to remove the surface inclusions introduced during the synthesis.

2.2. Sample characterization

The X-ray diffraction patterns were recorded on a Rigaku D/MAX 2250 V diffractometer with an operating voltage of 30 kV and current of 100 mA. The morphology and microstructure of annealed samples were investigated by transmission electron microscopy (TEM) on a JEOL JEM-2100F. The diffuse reflectance spectra (DRS) were obtained on a UV–vis spectrophotometer (Hitachi U-3010) using $BaSO_4$ as the reference. X-Ray photoelectron spectroscopy (XPS) analysis was performed on ESCALAB 250Xi (Thermo Scientific Ltd.). The C1 s was used to correct the charge effects. The photoluminance spectra (PL) were recorded at room temperature with a fluorescence spectrophotometer (F-4600, Japan). The Zeta potential was measured via Zeta potential analyzer (Malvern Instruments Zetasizer Nano ZS90). Infrared (IR) spectroscopy was recorded using a Burker Tensor 27 spectrometer. After accumulation of 64 scans, the spectra were collected with a solution of 4 cm^{-1}.

2.3. Electrochemical measurement

The electrochemical measurements were conducted with a CHI 660D electrochemical workstation (Shanghai Chenhua, China) using a standard three-electrode system. To make a working electrode, as-prepared samples (g-C_3N_4 and K—CN) were deposited on a FTO conductive support (1.5 × 1.5 cm). Briefly, ethanol solution containing 30 wt% powders was ultrasonically scattered for 15 min, and then spread on the FTO substrate. After several hours air drying, as-prepared electrodes were further treated in an oven at 80 °C for 30 min before ready for tests. The photocurrent of various electrodes was recorded with a scan rate of 5 mV/s from −0.4 V to 1.4 V (vs. SCE) in a 0.5 M Na_2SO_4 solution. The Mott-Schottky curves were recorded to study the electron band structure of both g-C_3N_4 and K—CN samples. The current–time (i–t) curves were collected at 0.4 V (vs. SCE) under the irradiation of a Xe lamp. Linear sweep voltammetry (LSV) were recorded from +0.2 V to −0.8 V (vs SCE) with a scan rate of 50 mV/s in O_2 saturated Na_2SO_4 electrolyte (0.5 M). Electrochemical impedance spectroscopy (EIS) measurements were employed to study the transportation and separation of photo-generated charge carriers. A 0.5 M Na_2SO_4 electrolyte containing 5 mmol of $Fe(CN)_6^{3-/4-}$ was applied.

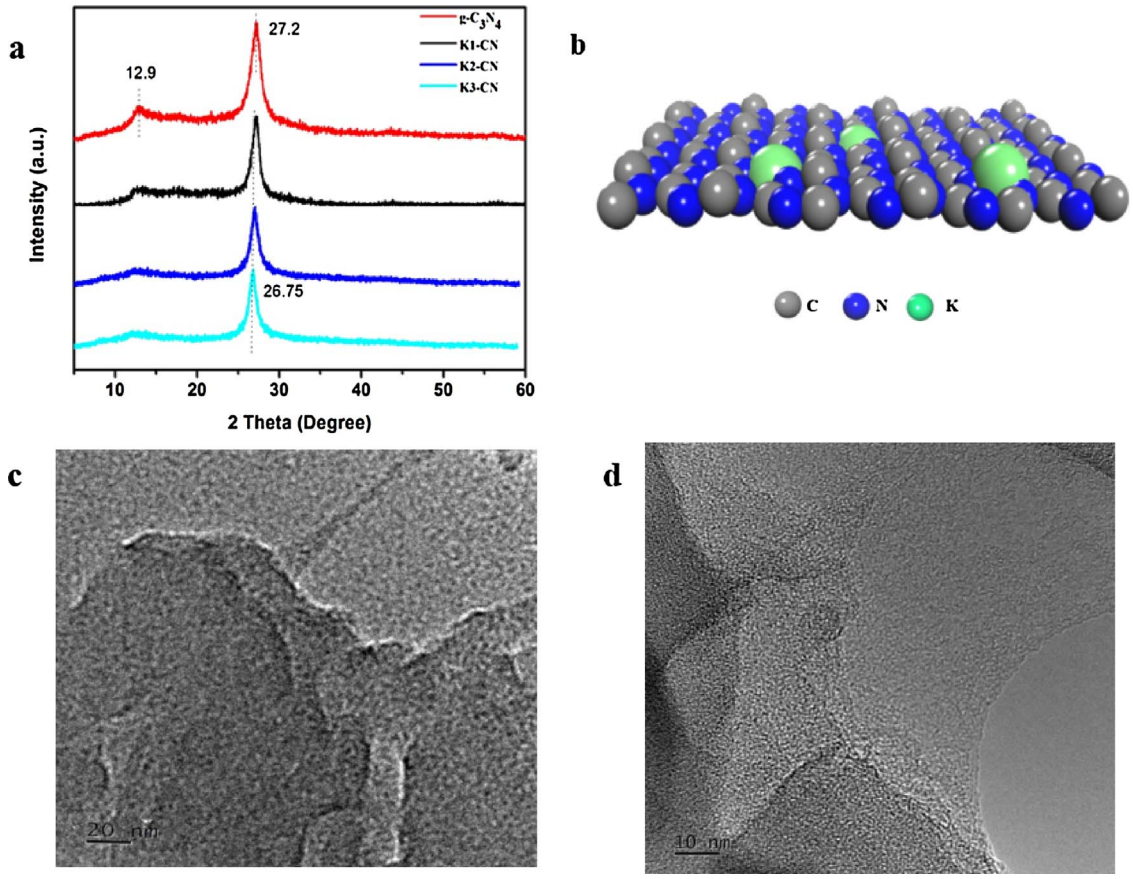

Fig. 1. (a) Crystal structure model of 1 K doped g-C_3N_4 optimized via the first principle; (b) XRD pattern of g-C_3N_4 and K—CN samples treated with different concentration of KOH solution, The blue, gray and purple balls represented N, C and K, respectively; (c) and (d) TEM image of irregular curved layers structure of pristine g-C_3N_4 and K3-CN sample. (For interpretation of the references to colour in this figure legend, the reader is referred to the web version of this article.)

2.4. Photocatalytic oxidation experiments

As-prepared samples were tested in photocatalytic oxidation of benzyl alcohol in ultrapure water at room temperature using a 500 W Xe lamp as the light source. Visible light irradiation was obtained using a 420 nm cut-off filter. Typically, powders (50 mg) were suspended in an aqueous solution of benzyl alcohol (100 mL, 0.5 mM) in a 200 mL gas-closed vitreous reactor, with a quartz window and a double walled jacket. Before light irradiation, above suspension was magnetically stirred for 1 h in the dark to reach an adsorption-desorption equilibrium between photocatalyst powders and benzyl alcohol. After 2 h irradiation, 2 mL of suspension were collected, followed by centrifugation and filtration using a 0.22 μm filter membrane. The concentration of residual benzyl alcohol, benzaldehyde and benzoin was decided using an Aligent TC-C18 high-performance liquid chromatography (HPLC). The conversion of benzyl alcohol and the selectivity for benzoin were defined as follows:

$$\text{Conversion rate}(\%) = (C_0 - C_{BA})/C_0 \times 100 \quad (1)$$

$$\text{Selectivity rate}(\%) = C_{Benzoin}/(C_0 - C_{BA})/C_0 \times 100 \quad (2)$$

where C_0 is the initial concentration of benzyl alcohol, and C_{BA} and $C_{Benzoin}$ are the concentration of benzyl alcohol and benzoin after a certain period of light irradiation, respectively.

The production of $\cdot O_2^-$ in K—CN and g-C_3N_4 suspensions was quantitatively analyzed by detecting the concentration of NBT in solution with UV–vis spectrophotometer. Briefly, various g-C_3N_4 (50 mg) were added into a 5×10^{-5} M NBT solution (100 mL). Prior to light irradiation, the suspension was stirred in the dark for 30 min. At given time intervals after irradiation, 4 mL of the suspension was collected and centrifuged to remove the catalyst powders. Hydrogen peroxide (H_2O_2) formation in the reaction system was measured via a (*p*-hydroxyphenyl) acetic acid (POHPAA) analysis method. Typically, a certain volume of fluorescence reagent (potassium hydrogen phthalate: 8.2 g/L, *p*-hydroxyphenylacetic acid: 270 mg/L, and type II horseradish peroxidase: 30 mg/L) was added into the reaction system in advance. 1.0 mL of sample was withdrawn at given time intervals and then mixed with 1.0 mL of 1.0 M NaOH for 10 min. The intensity of the fluorescence emission at 409 nm with an excitation of 315 nm light was detected. The formation of the hydroxyl radical on the surface of the K3-CN and g-C_3N_4 samples under UV–vis irradiation was monitored by the PL technique with terephthalic acid (TA) (5×10^{-4} M in 2×10^{-3} NaOH solution) as a probe molecule. The fluorescence spectra of the formed 2-hydroxyterephthalic acid from TA were measured by a spectrophotometer (Hitachi F-4500) excited at 315 nm.

In order to explore the active species during photocatalytic oxidation of benzyl alcohol, oxalic acid (5 mL), NBT (2×10^{-5} mol/L) and isopropanol alcohol (5 mL) were added to reaction system to capture the photo-induced holes, $\cdot O^{2-}$ and $\cdot OH$.

2.5. Calculation

Theoretical calculation Mullikan population analysis were carried out using CASTEP program package, working in a plan wave basis set within the framework of the projector augmented wave (PAW) method. The Perdew-Burke-Ernzerhof (PBE) exchange-correlation function was used within the spin-polarized generalized gradient approximation (GGA).The Brillouin zones of the supercells were sampled by a grid of $3 \times 3 \times 1$ (g-C_3N_4 and K—CN) K-points. The cutoff energy was 450 eV and the ultrasoft pseudo potential was used to describe the interaction

between valence electrons and ionic core. A single K atom was introduced into the 1 × 1 × 2 supercell of pristine g-C_3N_4 via the interstitial modification ways as reported. The geometry optimizations were performed under the electron wave function with expansion in plane wave to a cutoff energy of 310 eV, the Monkhorst − Pack k-point mesh of 2 × 2 × 1 and the self-consistent field of 2 × 10^{-6} eV/atom, 0.05 GPa for maximal stress and 0.001 Å for max. The atomic relaxations were conducted until the residual force was smaller than 0.05 eV/Å.

3. Results and discussion

3.1. Characterization

Successful surface alkaline modification was firstly confirmed via X-ray diffraction (XRD) analysis (Fig. 1a). Compared with the XRD pattern of pristine g-C_3N_4 (JCPDS 87-1256), K^+ introduction induced the shift of (002) characteristic peak from 27.2° to 26.8°, indicating increased interlayer spacing of lamellar g-C_3N_4. Furthermore, the much weaker (100) diffraction peak at 12.9° of K3-CN suggested that K^+ intercalation notably destroyed the periodic structure and caused the attractive interaction between K and N atoms [19]. The simulation model of K modified g-C_3N_4 (K-CN) is shown in Fig. 1b. The K atom was located in the layers of g-C_3N_4. Hereinafter for succinct description, K3-CN is selected as representative for detailed discussion and comparison with pristine g-C_3N_4. The morphology of pristine and modified g-C_3N_4 was studied via transmission electron microscopy (TEM). As shown in Fig. 1c and d, the microscopic morphology nearly kept unchanged after K^+ modification.

The K^+ modification can be further verified by flourier transform infrared spectroscopy (FTIR). As indicated in Fig. 2a, the absorption peak around 3303 cm^{-1} is ascribed to H_2O and amino groups from residual organic fragments in g-C_3N_4, while peaks located from 1200 to 1650 cm^{-1} are assigned to C≡N containing species [21]. Notably, after K^+ ions introduction, the peak intensity around 3303 cm^{-1} significantly decreased, implying the substitution of H sites in amino groups by K atoms [21]. Besides, damage of g-C_3N_4 framework can also be confirmed by the weakened absorption band for K−CN in the range of 1200 ~ 1650 cm^{-1}, in accordance with the decreased (100) diffraction peak (Fig. 1b).

In order to further reveal the interactions between intercalated K^+ and g-C_3N_4, both samples were carefully studied by X-ray photoelectron spectroscopy (XPS). In Fig. S1, compared to the silent signal of pristine g-C_3N_4, K 2p response is obviously detected in K3-CN, indicating successful introduction of K. Furthermore, K3-CN displays two K 2p core level components at 292.6 eV (K $2p_{3/2}$) and 295.5 eV (K $2p_{1/2}$), suggesting the presence of K atoms in the form of N−K bonds via substituting the H sites in amino groups from melamine or melen precursors [22]. As shown in Fig. 2b, high-resolution N 1 s spectrum of pristine g-C_3N_4 can be fitted into three sub peaks centered at 398.6 eV, 399.9 eV and 401.1 eV, which are ascribed to the tertiary carbon C−N−C, hybridized sp^3 N with bonding hydrogen and N−H bonding, respectively. Notably after K modification, the characteristic peaks of two kinds of N−H bonding at 399.9 eV (C−NH_x species) and 401.1 eV (C−N−H species) disappeared in K3-CN, accompanied with the formation of a new peak of C−N_3 bonding at 400.7eV [23]. This trend clearly suggests the deprotonation effect of K^+ modification, that is, the substitution of H in amino groups by K [18]. Above speculation agrees well with the results from FTIR analysis. In contrast as shown in Fig. 2c, the C 1s spectra of g-C_3N_4 and K−CN are nearly the same with no recognizable peak shift after K^+ introduction, suggesting relatively weak interaction between K and C atoms. According to above FTIR and XPS

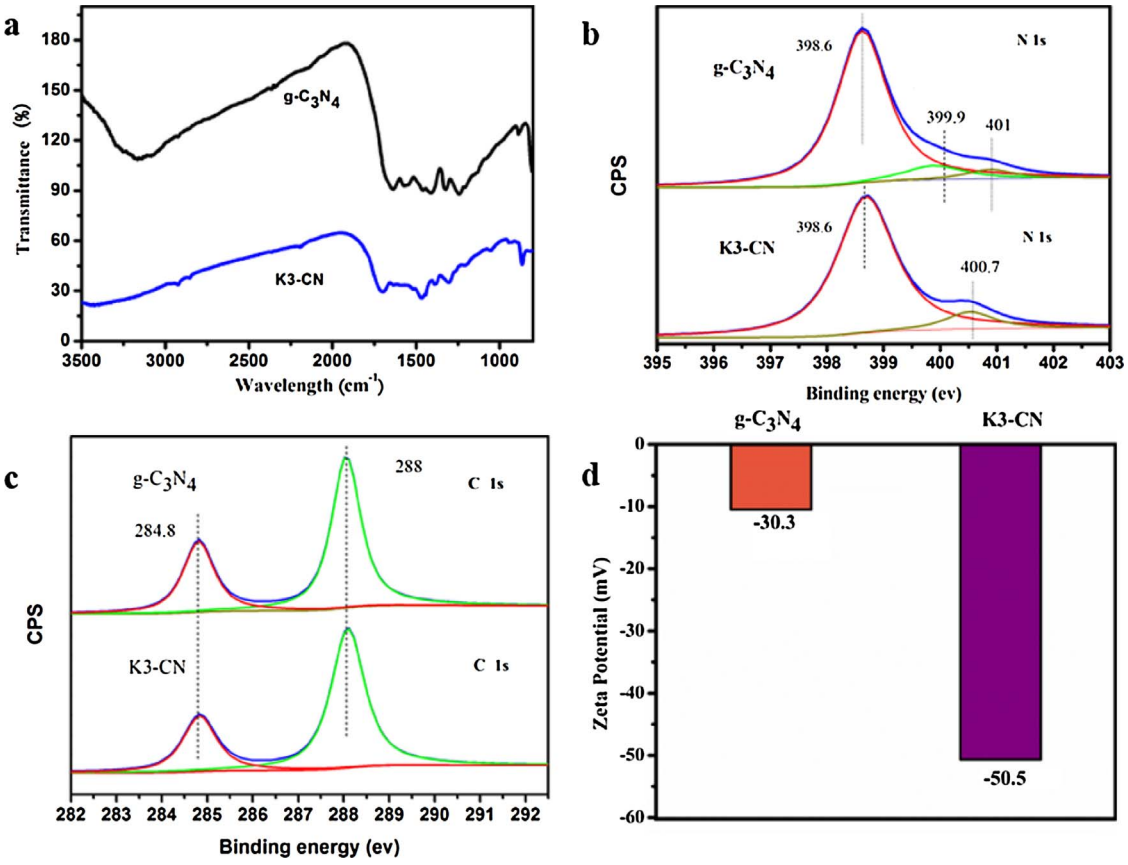

Fig. 2. (a) FTIR spectra of g-C_3N_4 and K3-CN; (b) High-resolution XPS spectra in N 1s and C 1s; (c) regions of g-C_3N_4 and K3-CN; (d) Zeta Potential of g-C_3N_4 and K3-CN measured in H_2O (pH = 7).

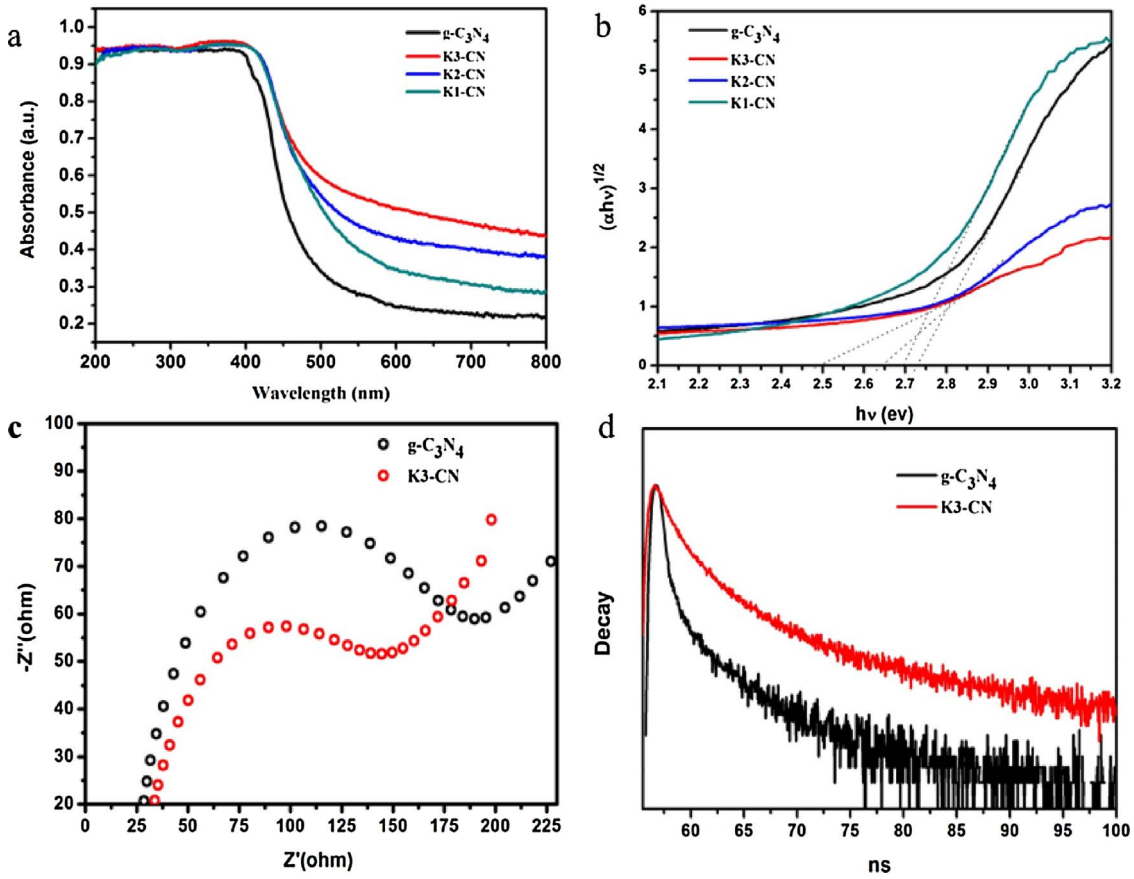

Fig. 3. (a) UV–vis diffuse reflectance spectrum of as-prepared g-C_3N_4 and various K—CN sample; (b) Estimated energy gap of g-C_3N_4 and various K—CN samples; (c) EIS Nyquist plots over g-C_3N_4 and K3-CN under the full spectra of Xe-lamp;(d) Time-resolved fluorescence decay spectra of different CNs monitored at 520 nm, by time-correlated single-photo counting. The samples were excited by the incident light of 280 nm.

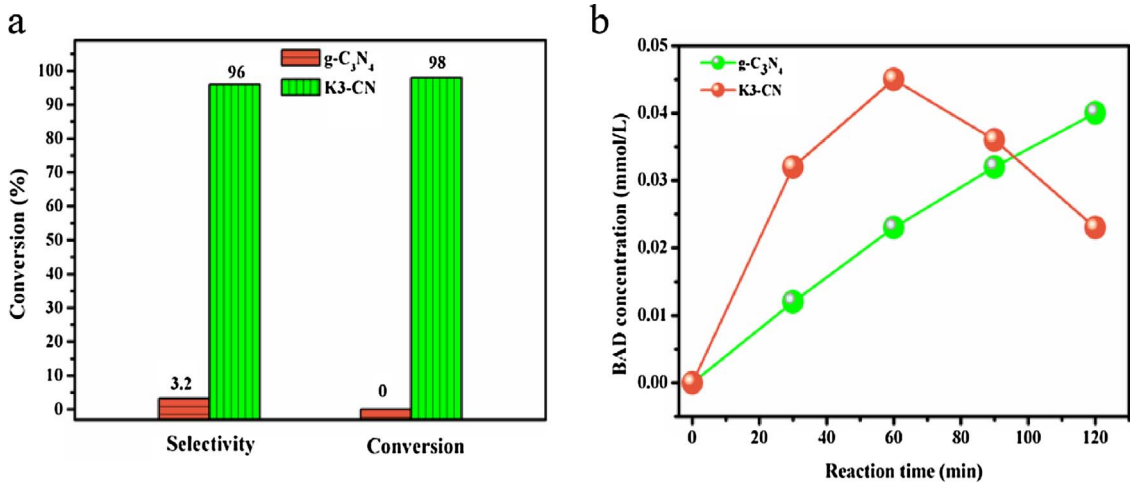

Fig. 4. (a) Photocatalytic benzyl alcohol conversion and benzoin selectivity over pristine g-C_3N_4 and K3-CN; (b) Evolution of intermediate benzaldehyde in the reaction system during 2 h period.

analysis, successful partial substitution of amino H by K can be concluded. As shown in Fig. 2d, the zeta potentials of pristine g-C_3N_4 and K3-CN dispersed in water (pH = 7) were determined to be −30.3 mV and −50.5 mV, respectively. This substantial potential change implied that K^+ introduction changed the g-C_3N_4 surface to be more negative charged, which should be favorable for the combination with the carbonium within the carbonyl groups of intermediate benzaldehyde [24].

For photocatalysts, both optical absorption and charge transport within it are important factors. For this respect, UV–vis diffuse reflection spectrum (DRS) and electrochemical impedance spectroscopy (EIS) were conducted (Fig. 3). As indicated in Fig. 3a, compared to pristine g-C_3N_4, the photo-absorption of which nearly disappears beyond 470 nm, K—CN series samples present obvious red-shift of absorption edge to 500 nm. According to the band gap estimation using the Kubelka–Munk equation, after K^+ modification, the band gap of g-C_3N_4 decreased from 2.67 eV to 2.45 eV (shown in Fig. 3b). Nyquist plots of g-C_3N_4 and K3-CN electrodes obtained from impedance measurements are shown in Fig. 3c. Notably, under light irradiation, K3-CN

presented a much smaller semicircle in the high-frequency region than that of the pristine g-C_3N_4, indicating promoted separation and transport of photogenerated carriers. As shown in Fig. 3d, using the time-resolved flourescence decay spectroscopy, above conclusion can be further confirmed by the prolonged lifetime of charge carriers within K3-CN upon suitable light excitation. With no doubt, much enhanced optical absorption and charge transport will be favorable for photocatalytic processes over K^+ modified C_3N_4.

3.2. Photocatalytic benzoin synthesis

Light-driven benzoin synthesis from benzyl alcohol was studied over g-C_3N_4 and K—CN under Xe lamp irradiation. As shown in Fig. 4a, the conversion of benzyl alcohol as well as the selectivity towards benzoin was recorded. Obviously compared to pristine g-C_3N_4, alkalinized K—CN samples present significantly enhanced conversion and selectivity. After irradiation for 2 h, the conversion and selectivity over K3-CN reached 95.3% and 93.2%, while for pristine g-C_3N_4 the two values were only 6.3% and 4.3%, respectively. Under visible light ($\lambda > 420$ nm) irradiation, the conversion and selectivity over g-C_3N_4 still reach 67.7% and 64.5%, as shown in Fig. S2a. The conversion and selectivity over different K^+ modified samples were also studied (shown in Fig. S2b). All of the K^+ modified samples show the selectivity to benzoin and the selectivity was further optimized with the increasing amount of K^+. Furthermore, the cycling stability of K3-CN in benzoin synthesis was further studied under Xe lamp irradiation (Fig. S2c). After 5 continuous cycles, the benzyl alcohol conversion as well as the selectivity for benzoin nearly kept unchanged, indicating excellent cycling stability of K^+ modified g-C_3N_4 photocatalyst.

During the whole light-induced process, no by-product other than benzaldehyde was detected, which probably was the intermediate. In order to verify this point, we monitored the evolution of benzaldehyde over time during photocatalytic benzoin production. As shown in the inset of Fig. 4b, the benzaldehyde concentration in pristine g-C_3N_4 system showed continues increase during the two hours reaction period. However, for K—CN system, the benzaldehyde concentration increased in the first 60 min and decreased as prolonged irradiation continued. This trend clearly indicated that there existed an accumulation of benzaldehyde at the beginning, followed by the consumption of benzaldehyde when the evolution of benzoin exceeded that of benzaldehyde, confirming benzaldehyde as the intermediate during benzyl alcohol conversion to benzoin. Furthermore, photocatalytic benzoin condensation was also tested using benzaldehyde as starting material. Similarly as shown in Fig. S2d, K3-CN presented much enhanced conversion rate of benzaldehyde (90.2%) and selectivity towards benzoin (97%), compared to only 3.2% and 0.1% for the pristine g-C_3N_4.

3.3. Enhanced production of reactive oxidative species

Photocatalytic organics conversion is usually driven by oxidative intermediates, such as superoxide radical ($\cdot O_2^-$), hydroxyl radical ($\cdot$OH), hydrogen peroxide (H_2O_2), and so forth. In this respect, enhanced production of oxidative species can be expected over alkaline modified g-C_3N_4 K—CN, due to the enhanced photo-absorption and charge transport as discussed above. Firstly, linear sweep voltammogram (LSV) was used to investigate the O_2 reduction ability over different samples. Fig. 5a presents LSV of g-C_3N_4 and K—CN electrodes measured in the O_2 saturated electrolyte solution. Notably, K—CN electrode presented greatly enhanced cathodic current when compared to that of the pristine g-C_3N_4 one, indicating that K^+ modification makes the molecular O_2 reduction over g-C_3N_4 surface much easier [25,26]. Furthermore, photo-degradation of nitroblue tetrazolium (NBT) was conducted to evaluate the production of superoxide radicals ($\cdot O_2^-$) over two samples under light excitation. According to the Mott-Schottky plots (shown in Fig. S3), the conduction band minimum position of K3-CN (−1.63 eV vs SCE) is more negative than that of $^*O_2^-/O_2$ (−0.33 V vs SCE) and g-C_3N_4 (−1.13 eV vs SCE) respectively, which indicates the O_2 reduction ability of g-C_3N_4 is enhanced after K^+ modification. As shown in Fig. 5b, 97% of added NBT was consumed after 30 min in K-C_3N_4 contained solution, while for g-C_3N_4 only 20.3% was consumed even after 2 h irradiation. This result is in good coincidence with the conclusion obtained from the Oxygen Reduction Reaction (ORR) performance of two sample electrodes in Fig. 5a.

As a reduction product of O_2, H_2O_2 might also be produced within C_3N_4-based photocatalytic system [27–29]. In this study, photo-induced H_2O_2 formation was monitored via a (*p*-hydroxyphenyl) acetic acid (POHPAA) analysis method. As shown in Fig. 5c and d, H_2O_2 was not detected in the absence of either catalyst or light irradiation, indicating the photocatalytic nature of H_2O_2 production. Furthermore, O_2 is essential for the generation of H_2O_2 because no H_2O_2 was detected when O_2 is replaced by Ar. Notably in Fig. 5c, with Xe lamp irradiation, the H_2O_2 production of K3-CN (75 μmol) system is approximately 5 times higher than that of pristine g-C_3N_4 (15 μmol), further confirming much enhanced O_2 activation over K3-CN. As shown in Fig. 5d, in the presence of benzyl alcohol even higher H_2O_2 yield (153 μmol) over K—CN was observed after 2 h light irradiation, 2.5 times higher than that in pure water, indicating that the introduction of benzyl alcohol greatly enhanced the H_2O_2 production. This is probably because that benzyl alcohol itself can serve as proton source and thus enhance the H_2O_2 production via directly reacts with $\cdot O_2^-$, as indicated by Eq. (1) [30].

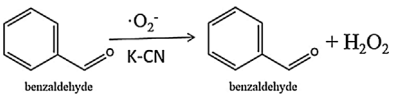

(1)

Furthermore, 2-hydroxy terephthalic acid (TA) was employed as a fluorescent probe to detect the presence of hydroxyl radicals ($\cdot$OH) in the g-C_3N_4 and K3-CN system. As shown in Fig. S4a and S4b , after 1 h illumination, the $\cdot$OH production in K3-CN system is approximately 2 times higher than that in the pristine g-C_3N_4 system.

The roles various oxygen-containing species play during photocatalytic benzoin synthesis were carefully studied. Firstly, the role of O_2 was studied via Ar replacement. Notably in Fig. S5, K3-CN presented only 5.3% conversion in the Ar-saturated system, clearly indicating the aerobic nature of this photo-driven process. The roles of holes (h^+), hydroxyl radicals ($\cdot$OH) and superoxide radical ($\cdot O_2^-$) were studied by adding corresponding scavengers. As shown in Fig. S5, the benzyl alcohol conversion presented slight decrease to 84.5% in the presence of isopropylalcohol (IPA) as $\cdot$OH scavenger, indicating that $\cdot$OH made minor contribution to this process. Besides, with addition of oxalic acid (OA) as h^+ scavenger benzyl alcohol conversion kept almost unchanged, indicating the negligible role of photo-generated h^+ in benzoin synthesis. In contrast, after scavenging $\cdot O_2^-$ using NBT, the benzyl alcohol conversion obviously decreased to 6.1%, clearly suggesting $\cdot O_2^-$ as the main active specie in benzoin synthesis. It is worth noting that, within all above conditions, the selectivity for benzoin kept almost unchanged (over 90%), suggesting that the oxidative species mainly influence the benzyl alcohol conversion, but not selective benzoin formation.

3.4. Possible mechanism

Given above discussion on benzaldehyde evolution, selective conversion of benzyl alcohol to benzaldehyde should be the first step during photocatalytic benzoin synthesis over g-C_3N_4. As confirmed in Results, under light excitation K—CN presented much enhanced production of $\cdot O_2^-$ and H_2O_2, which have been proved favorable for benzyl alcohol conversed to benzaldehyde, as indicated by Eqs. (2) and (3). As a result, compared to pristine g-C_3N_4, K—CN should possess superior ability in converting benzyl alcohol to benzaldehyde, in good coincidence with the results in Fig. 2.

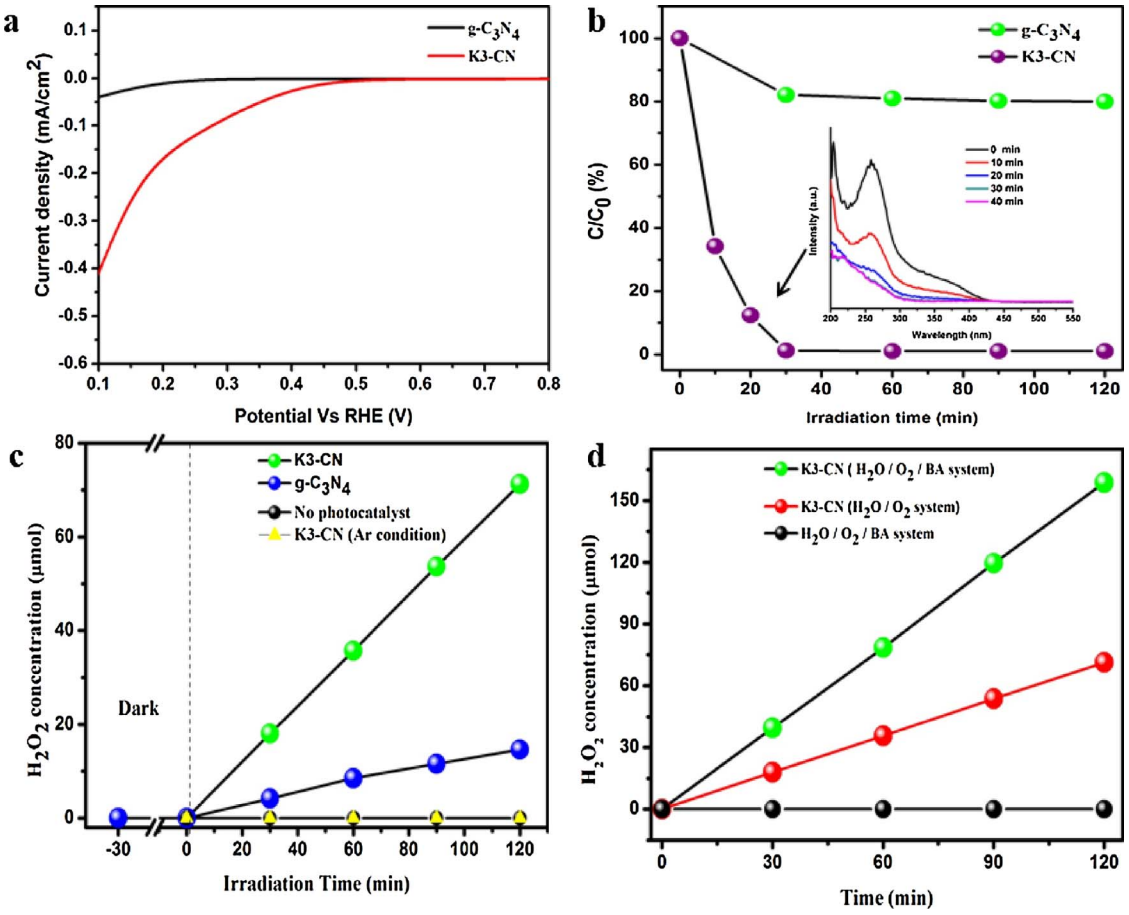

Fig. 5. (a) Linear sweep voltammetry (LSV) curves of pristine g-C_3N_4 and K3-CN electrodes measured in O_2-saturated Na_2SO_4 solution with a scan rate of 50 mV/s; (b) Evolution of NBT concentration within catalyst contained suspension; inset is UV–vis absorption spectra recorded with time; (c) production of H_2O_2 over g-C_3N_4 and K3-CN under Xe lamp irradiation; (d) production of H_2O_2 over K3-CN under controlled conditions.

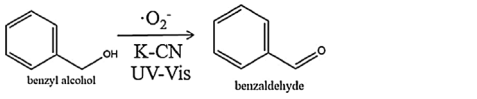

(2)

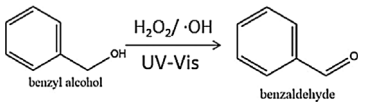

(3)

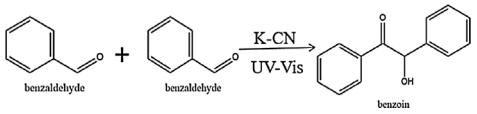

(4)

After selective benzyl alcohol conversion to benzaldehyde, oxidative C—C coupling between two benzaldehyde molecules is the second step for producing one benzoin molecule, as indicated in Eq. (4). In order to achieve efficient C—C coupling, umpolung of the carbonium ion of one benzaldehyde molecule is of crucial importance. Therefore, materials with nucleophilic surface properties could be potential candidate for catalyzing this process. As indicated by the zeta potential results, under reaction conditions (pH = 7), both g-C_3N_4 and K—CN are negatively surface charged and thus tend to combine with the carbonium ions within the carbonyl groups of intermediate benzaldehyde (Fig. 6).

For pristine g-C_3N_4, the lone pair electrons of residual amino nitrogen make it easy to form C—N connections with carbonyl carbon of benzaldehyde due to the electrostatic attraction, therefore greatly interrupting the C—C coupling for benzoin condensation [31]. For K—CN as discussed in Section 3.1, with K^+ introduction, amino H atoms could be successfully substituted by K, that is, the deprotonation of surface groups in g-C_3N_4, as shown in Fig. 4. In order to get in-depth insights into the deprotonation effect of K substitution, Mulliken populations of C, N and K atoms in both g-C_3N_4 and K—CN were calculated via augmented-wave (PAW) method. According to the computational results, after introducing K^+, the Mullikan charge of C decreased from +0.49 in g-C_3N_4 to +0.27 ~ + 0.47 in K—CN, meanwhile that of K increased from 0 in isolated K^+ ions to +2.58 in K—CN. Given that no obvious change of the Mullikan charge of N (−0.49) was observed, it can be concluded that there happened electrons transfer from exotic K^+ ions to skeletal C atoms within g-C_3N_4 during K^+ substitution. In other words, after K^+ modification C atoms are enriched by more delocalized electrons, that is, much enhanced nucleophilicity [32]. With remarkable nucleophilicity of K—CN, it is reasonable to expect more efficient umpolung of carbonium ions in benzaldehyde molecules via electron transfer from K—CN. More visually, photocurrent decay is another evidence to confirm the electron-rich surface of K—CN. As shown in Fig. S6, the apparent current decay of K—CN electrode last for 10 s while it is only 0.5 s for pristine g-C_3N_4, implying the increased possibility of free electrons transfer between the catalyst and the reactants. As a result, compared to pristine g-C_3N_4, much more efficient C—C coupling for benzoin condensation can be well clarified over K—CN, as indicated in Scheme 1.

4. Conclusion

In summary, efficient benzyl alcohol conversion into benzoin was achieved over alkalinized g-C3N4 (K—CN) photocatalyst with high selectivity. The light-driven benzoin synthesis consisted of selective benzyl alcohol conversion to benzaldehyde and successive C—C coupling between benzaldehyde. The superior benzoin production over

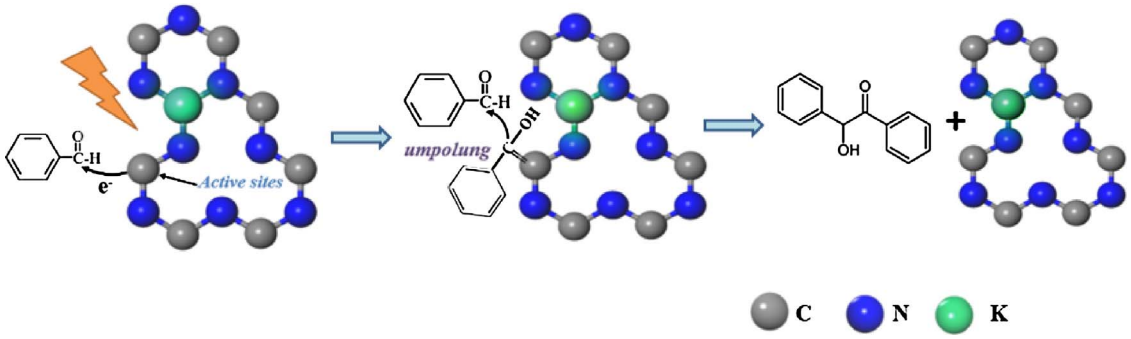

Fig. 6. Proposed reaction mechanism of photocatalytic benzoin synthesis over K−CN.

K−CN was attributed to the modifications of electronic structure as well as surface chemical environment in g-C_3N_4 induced by alkali treatment. Firstly, K+ intercalation facilitated the light harvesting of g-C_3N_4 as well as the transport and separation of photo-generated charge carriers. Secondly, K^+ modification induced effective deprotonation of g-C_3N_4 by substituting H atoms in surface amino groups. As a result, skeletal C in g-C_3N_4 is enriched by more delocalized electrons, presenting remarkable nucleophilicity and greatly prompting the C−C coupling reactions between benzaldehyde. Our results pave the way for simple and effective material optimization towards ideal solar energy utilization as well as for the green synthesis of benzoin over earth-abundant inorganic photocatalysts.

Acknowledgements

We acknowledge the financial support from the 973 Program (2013CB933200) and National Natural Science Foundation of China (51472260)

Appendix A. Supplementary data

Supplementary data associated with this article can be found, in the online version, at http://dx.doi.org/10.1016/j.apcatb.2017.08.057.

References

[1] J. Du, H. Singh, T.H. Yi, Bioprocess. Biosyst. Eng. 39 (2016) 1923–1931.
[2] G. Zhang, S. Yang, X. Zhang, Q. Lin, D.K. Das, J. Liu, X. Fang, J. Am. Chem. Soc. 138 (2016) 7932–7938.
[3] P. Burger, A. Casale, A. Kerdudo, T. Michel, R. Laville, F. Chagnaud, X. Fernandez, Food Chem. 210 (2016) 613–622.
[4] E. Frick, C. Schweigert, B.B. Noble, H.A. Ernst, A. Lauer, Y. Liang, D. Voll, M.L. Coote, A.-N. Unterreiner, C. Barner-Kowollik, Macromolecules 49 (2016) 80–89.
[5] J.H. Lee, J.H. Jang, N. Velusamy, H.S. Jung, S. Bhuniya, J.S. Kim, Chem. Commun. (Camb.) 51 (2015) 7709–7712.
[6] Y. He, Y. Xue, J. Phys. Chem. A 114 (2010) 9222–9230.
[7] N. Marion, S. Diez-Gonzalez, S.P. Nolan, Angew. Chem. Int. Ed. 46 (2007) 2988–3000.
[8] R. Matsubara, S. Kobayashi, Acc. Chem. Res. 41 (2008) 292–301.
[9] S.E. Denmark, T.W. Wilson, Angew. Chem. Int. Ed. 51 (2012) 9980–9992.
[10] B. Maji, M. Breugst, H. Mayr, Angew. Chem. Int. Ed. 50 (2011) 6915–6919.
[11] Y. Shimakawa, T. Morikawa, S. Sakaguchi, Tetrahedron Lett. 51 (2010) 1786–1789.
[12] X. Lang, X. Chen, J. Zhao, Chem. Soc. Rev. 43 (2014) 473–486.
[13] D. Tsukamoto, Y. Shiraishi, Y. Sugano, S. Ichikawa, S. Tanaka, T. Hirai, J. Am. Chem. Soc. 134 (2012) 6309–6315.
[14] H. Su, K.X. Zhang, B. Zhang, H.H. Wang, Q.Y. Yu, X.H. Li, M. Antonietti, J.S. Chen, J. Am. Chem. Soc. 139 (2017) 811–818.
[15] L. Moehlmann, S. Blechert, Adv. Synth. Catal. 356 (2014) 2825–2829.
[16] Y. Wang, X. Wang, M. Antonietti, Angew. Chem. Int. Ed. 51 (2012) 68–89.
[17] T. Sano, S. Tsutsui, K. Koike, T. Hirakawa, Y. Teramoto, N. Negishi, K. Takeuchi, J. Mater. Chem. A 1 (2013) 6489–6496.
[18] F. Guo, J. Chen, M. Zhang, B. Gao, B. Lin, Y. Chen, J. Mater. Chem. A 4 (2016) 10806–10809.
[19] Y. Li, S. Ouyang, H. Xu, X. Wang, Y. Bi, Y. Zhang, J. Ye, J. Am. Chem. Soc. 138 (2016) 13289–13297.
[20] N. Tian, Y. Zhang, X. Li, K. Xia o, X. Du, F. Dong, G.I.N. Waterhouse, T. Zhang, H. Huang, Nano Energy 38 (2017) 72–81.
[21] Q. Guo, Y. Zhang, J. Qiu, G. Dong, J. Mater. Chem. C 4 (2016) 6839–6847.
[22] T. Xiong, W. Cen, Y. Zhang, F. Dong, ACS Catal. 6 (2016) 2462–2472.
[23] X. Yuan, C. Zhou, Y. Jin, Q. Jing, Y. Yang, X. Shen, Q. Tang, Y. Mu, A.K. Du, J. Colloid Interface Sci. 468 (2016) 211–219.
[24] B. Wang, M. Lin, T.P. Ang, J. Chang, Y. Yang, A. Borgna, Catal. Commun. 25 (2012) 96–101.
[25] S. Li, G. Dong, R. Hailili, L. Yang, Y. Li, F. Wang, Y. Zeng, C. Wang, Appl. Catal. B 190 (2016) 26–35.
[26] B. Zhang, S. Wang, W. Fan, W. Ma, Z. Liang, J. Shi, S. Liao, C. Li, Angew. Chem. Int. Ed. Engl. 55 (2016) 14748–14751.
[27] Z. Wan, G. Zhang, X. Wu, S. Yin, Appl. Catal. B 207 (2017) 17–26.
[28] D. Tang, G. Zhang, Appl. Surf. Sci. 391 (2017) 415–422.
[29] H. Huang, S. Tu, C. Zeng, T. Zhang, A.H. Reshak, Y. Zhang, Angew. Chem. (2017), http://dx.doi.org/10.1002/ange.201706549.
[30] P. Ferreira, A. Hernandez-Ortega, B. Herguedas, J. Rencoret, A. Gutierrez, M.J. Martinez, J. Jimenez-Barbero, M. Medina, A.T. Martinez, Biochem. J. 425 (2010) 585–593.
[31] J.E. Perez, M. Kumar, J.S. Francisco, A. Sinha, J. Phys. Chem. A 121 (2017) 1022–1031.
[32] K. Ranjan, K. Dharamvir, V.K. Jindal, Phys. B-Condens. Matter 365 (2005) 121–133.